Dense plasma microfield nonuniformity

M. S. Murillo, D. P. Kilcrease, and L. A. Collins
Theoretical Division, Los Alamos National Laboratory, Los Alamos, New Mexico 87545
(Received 25 October 1996)

Plasma microfield-constrained-average quantities arise in a variety of applications including the ion quadrupole effect, the ion motion problem, and autoionizing processes. We critically compare several methods for computing such quantities in the context of microfield-constrained field gradients, which are used for describing the ion quadrupole effect, a source of spectral line asymmetry. Specifically, we show that one adjustable parameter exponential approximation (APEX)-like theory is divergent and compare existing nearest-neighbor models, APEX, and Monte Carlo results. Moreover, we have performed molecular-dynamics simulations to assess the accuracy of these previous results. Our results indicate that APEX calculations of this particular constrained average are quite accurate except at large field values, which are unimportant for line shapes. Interestingly, nearest-neighbor results are quite accurate for certain field gradients and not for others. [S1063-651X(97)05705-X]

PACS number(s): 52.25.Gj, 52.65.−y, 52.70.La

I. INTRODUCTION

Atomic emission and absorption spectral line shapes are useful as density and temperature diagnostics in plasmas [1]. Often the effects of all of the perturbing plasma ions on an atom can be treated as a uniform plasma electric microfield [2]. For dense plasmas, however, microfield nonuniformities due to electric-field gradients must be considered since they contribute to line asymmetries [3–6]. This effect can be formulated in terms of the microfield-constrained average of the components of the spatial derivative of the microfield. The present paper presents a critical evaluation of this constrained average. This study also serves as an evaluation of an important approximation to the microfield-constrained radial distribution function $g(\mathbf{r};\boldsymbol{\epsilon})$. This quantity is used in the evaluation of constrained averages and gives the average perturber distribution at $\mathbf{r}$ around a radiator experiencing a field $\boldsymbol{\epsilon}$. These constrained averages are also applicable to the calculation of the time derivative of the electric microfield [7,8] and of microfield effects on the continuum wave functions involved in autoionizing processes [9].

In this paper we examine the average field-gradient theory of Kilcrease *et al.* [5] and compare it with accurate molecular-dynamics (MD) simulations. These results are compared with unscreened and screened nearest-neighbor (NN) models. We also discuss the divergence of the theory of Demura *et al.* [6,8].

II. THEORY

The constrained quantity $\langle \partial_{x_j} E_i \rangle_\epsilon$ is the ensemble average of all plasma ion configurations that produce a microfield $\boldsymbol{\epsilon}$ at the ion in question. $\partial_{x_j} E_i$ is the derivative of the ith component of the plasma microfield in the x_j direction at the ion, assuming the z axis is in the direction of the plasma microfield $\boldsymbol{\epsilon}$. An ion quasiparticle model based on Debye-Hückel (DH) pairwise interactions between identical ions is assumed with the interaction energy between ions i and j given by

$$V_{ij}(\mathbf{r}_i,\mathbf{r}_j) = [(Ze)^2/|\mathbf{r}_i-\mathbf{r}_j|]\, e^{-\kappa|\mathbf{r}_i-\mathbf{r}_j|}, \tag{1}$$

where $\kappa^2 = 4\pi n_e e^2/k_B T$, Z is the effective ion charge, and n_e is the electron number density.

The constrained average at a radiator of charge Z can be expressed as [5]

$$\langle \partial_{x_j} E_i \rangle_\epsilon = n_i \int d\mathbf{r}\, \partial_{x_j} E_i(r)\, g(\mathbf{r};\boldsymbol{\epsilon}), \tag{2}$$

where $\partial_{x_j} E_i = \Sigma_{k=1}^{N} \partial_{x_j} E_i(\mathbf{r}_k)$ for N total perturbing ions and

$$\partial_{x_j} E_i(r) = Ze\,\frac{e^{-\kappa r}}{r^3}\left\{\left(\delta_{ij} - 3\frac{x_i x_j}{r^2}\right)(1+\kappa r) - \kappa^2 x_i x_j\right\}. \tag{3}$$

In a previous work [5], Eq. (3) was approximated by neglecting terms proportional to κ^2. These terms are of the order of the charge density at the radiator due to the perturbing-ion screening clouds. In the present work, these terms are retained for consistency with the MD simulations.

Kilcrease *et al.* [5] showed that

$$g(\mathbf{r};\boldsymbol{\epsilon}) = \frac{1}{Q(\boldsymbol{\epsilon})}\int \frac{d\boldsymbol{\lambda}}{(2\pi)^3} e^{-i\boldsymbol{\lambda}\cdot\boldsymbol{\epsilon}} \widetilde{Q}(\boldsymbol{\lambda})\widetilde{g}(\mathbf{r};\boldsymbol{\lambda}), \tag{4}$$

where

$$\widetilde{g}(\mathbf{r};\boldsymbol{\lambda}) = (1/n_i)\,\{\delta G[\phi]/\delta(i\boldsymbol{\lambda}\cdot\mathbf{E}(r))\}. \tag{5}$$

Here $G[\phi] = \ln\widetilde{Q}(\boldsymbol{\lambda}) = \ln\langle e^{i\boldsymbol{\lambda}\cdot\mathbf{E}}\rangle$ is the microfield generating functional, $Q(\boldsymbol{\epsilon})$ is the microfield probability function, and n_i is the ion number density. This relation is exact and shows that the constrained average is derivable from a functional derivative of the microfield generating functional. Therefore, we can use an approximation for the generating function that will lead to a corresponding approximation to the constrained average. Use of the adjustable parameter exponential approximation (APEX) microfield generating functional [10] leads to [5,11]

$$\widetilde{g}(\mathbf{r};\boldsymbol{\lambda}) = g(r)\, e^{i\boldsymbol{\lambda}\cdot\mathbf{E}^*(r)}, \tag{6}$$

where $E^*(r)$ is the single-particle APEX screened field with the inverse screening length given by the adjustable screening parameter α and $g(r)$ is the radial distribution function.

This approximation to $\tilde{g}(\mathbf{r};\boldsymbol{\lambda})$ leads to a constrained average that obeys the expected normalization condition $\langle 1\rangle_\epsilon = 1$, a consequence of Eq. (6) satisifying the zeroth moment condition discussed in Ref. [11].

Another approximation to the constrained average is given by Demura *et al.* [6],

$$\tilde{g}(\mathbf{r};\boldsymbol{\lambda}) = g(r)\,[E(r)/E^*(r)]e^{i\boldsymbol{\lambda}\cdot\mathbf{E}^*(r)}, \tag{7}$$

where $E(r)$ is the single-particle DH screened field. This approximation arises from the use of an ''effective'' radial distribution function $G(r)$ defined by the APEX local-field constraint $E^*(r)G(r) = E(r)g(r)$ [10]. However, $G(r)$ is *not* a radial distribution function [12] and occurs as the result of renormalizing the Baranger-Mozer series expansion of $G(\boldsymbol{\lambda})$ in terms of an effective field $E^*(r)$. This renormalization leads, in a natural way, to the APEX second moment condition as well as the local-field constraint and it is therefore not necessary to define an effective radial distribution function. The use of $G(r)$ in Eq. (7) leads to a constrained average that violates the normalization condition $\langle 1\rangle_\epsilon = 1$, as seen by examining the radial part of $\langle 1\rangle_\epsilon$, viz.,

$$\frac{4\pi}{V}\int dr r^2 \frac{E(r)}{E^*(r)} g(r) j_0(\lambda E^*(r)), \tag{8}$$

where the radial integration is over the system volume V. For large r, $g(r)$ and the spherical Bessel function $j_0(\lambda E^*(r))$ go to unity but the ratio $E(r)/E^*(r)$ depends on the adjustable APEX screening parameter α and is proportional to $\exp[(\alpha-\kappa)r]$. For $\alpha/\kappa > 1$, the ratio and the normalization diverge exponentially, while for $\alpha/\kappa < 1$ the ratio goes to zero exponentially and the normalization is less than one. For $\alpha = \kappa$ the normalization condition is satisfied, but this corresponds to the independent particle model of Joyce *et al.* [4] and would not be expected to take proper account of perturber ion-ion interactions. As an example consider a pure Ar^{+17} plasma at temperature $k_B T = 800$ eV with $n_e = 1\times10^{23}$, 1×10^{24}, and 1×10^{25} cm^{-3} and find $\alpha/\kappa =$ 2.7, 2.3, and 1.9, respectively. The normalization of $g(\mathbf{r};\boldsymbol{\epsilon})$ using the approximation of Eq. (7) for $\tilde{g}(\mathbf{r};\boldsymbol{\lambda})$ will diverge for all three cases. Calculation of $\langle \partial_z E_z\rangle_\epsilon$ using this theory will lead to divergence for $\alpha/\kappa > 2$ due to an additional exponential factor from the field derivative. Due to these problems with the normalizability, Eq. (7) is generally not useful for evaluation of constrained averages.

Knowledge of $\langle \partial_z E_z\rangle_\epsilon$ and $\langle \partial_x E_x\rangle_\epsilon$ suffices to determine all field-gradient quantities since $\nabla\cdot\mathbf{E} = 4\pi\rho$. When the plasma microfield at the radiator is small, the term proprotional to κ^2 in Eq. (3) results in $\langle \partial_{x_i} E_i\rangle_\epsilon$ remaining finite as $\epsilon\to 0$, in contrast to Ref. [5]. For $i \neq j$, $\langle \partial_{x_j} E_i\rangle_\epsilon$ is always zero. On the other hand, when the plasma microfield at a radiator is very large, the field is dominated by a single perturber, the nearest neighbor. This suggests a simple model based on the nearest neighbor alone, which is valid for large field values. Locating the origin on the radiator and taking the perturber to be on the positive z axis, the magnitude of the electric field at the radiator is then

$$E(z) = (Zr_e^2/z^2)\,e^{-\kappa z}(1+\kappa z). \tag{9}$$

It is worth noting that this gives a prescription for computing $g(\mathbf{r},\boldsymbol{\epsilon})$. For a given field value $\boldsymbol{\epsilon} = E(z)$, the *single* particle is located at z. The field gradients are

$$\partial_z E_z(z) = -\frac{2Zr_e^3}{z^3}e^{-\kappa z}\left(1+\kappa z+\frac{1}{2}\kappa^2 z^2\right),$$

$$\partial_x E_x(z) = \frac{Zr_e^3}{z^3}e^{-\kappa z}(1+\kappa z), \tag{10}$$

where all electric fields are normalized by e/r_e^2 and electric-field derivatives are normalized by e/r_e^3, where the electron sphere radius $r_e = (3/4\pi n_e)^{1/3}$. These equations can be implicitly used to approximate the field gradient for a given value of the electric field in the high-field limit.

Plasma screening can be neglected if the perturber approaches the radiator at a distance much less than the screening length [5]. In this case the above equations take the simpler forms of

$$\partial_z E_z^{\rm NS} = -(2/\sqrt{Z})\,\epsilon^{3/2}, \quad \partial_x E_x^{\rm NS} = -\tfrac{1}{2}\,\partial_z E_z^{\rm NS}. \tag{11}$$

The superscript ''NS'' refers to the no-screening case.

III. MOLECULAR-DYNAMICS IMPLEMENTATION

MD calculations have been performed with various particle numbers in both the microcanonical and isokinetic ensembles. Periodic boundary conditions were used in all cases with the minimum image cell convention employed in computing the forces [13]. This convention, in contrast to the familiar Ewald procedure, is applicable as a result of the short-range nature of the interaction potential of Eq. (1). Time propagation was implemented by numerically integrating the coupled equations of motion using the velocity-Verlet algorithm [14]. The time step Δt was chosen relative to the plasma frequency ω_i such that $\omega_i \Delta t = 0.017$ and 0.054 for $n_e = 10^{24}$ and 10^{25} cm^{-3}, respectively.

Since it is necessary to perform MD simulations with a finite number of particles, results obtained are not performed in the thermodynamic limit and are subject to boundary effects. These effects, statistical ensemble dependence and system size, were investigated by varying the particle number in both microcanonical and isokinetic implementations. The microcanonical ensemble was sampled by accurately solving the exact equations of motion. Such a procedure exactly conserves energy in the limit that the time step approaches zero. Sampling from the isokinetic ensemble was achieved by a standard velocity scaling procedure, which ensures that the velocity distribution is consistent with the desired temperature at each time step [13].

Convergence of the MD with respect to particle number was tested with microfield calculations at $n_e = 10^{24}$ cm^{-3}. The results, performed in the isokinetic ensemble, are shown in Fig. 1 for $N = 54$ and $N = 686$ particles. Qualitatively, there is good agreement between the various calculations. An error parameter is defined as the rms value of

$$[P_{686}(\epsilon) - P_N(\epsilon)]/P_{686}(\epsilon)\times 100, \tag{12}$$

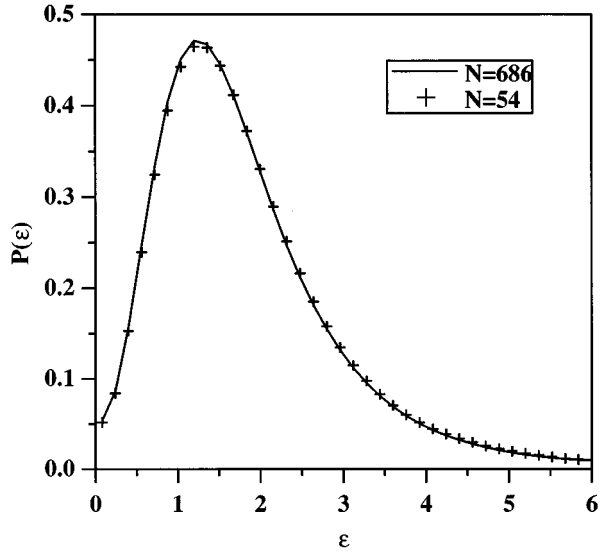

FIG. 1. Microfield distributions for $N=54$ and $N=686$ particles. The simulation was carried out in the isokinetic ensemble at 800 eV and $n_e=10^{24}$ cm^{-3} for $Z=17$. Note that $P(\epsilon)=4\pi\epsilon^2 Q(\epsilon)$. The electric field ϵ is measured in units of e/r_e^2.

where $N=54$, 250, and 432. This parameter is a measure of the error relative to the most accurate simulation performed. The rms errors over the range $\epsilon=0-6$ were found to be 3.4% for $N=54$, 1.1% for $N=250$, and 0.9% for $N=432$. As such, we feel that the $N=250$ case is adequate for distinguishing among the various analytical models for microfields.

The ensemble dependence was explored with the field-gradient calculations for various numbers of particles. Since the MD simulations are performed in the laboratory frame, the field gradients were rotated such that the z axis lies in the direction of the plasma microfield $\boldsymbol{\epsilon}$. The results are shown in Fig. 2 for $n_e=10^{24}$ cm^{-3}. The MD field-gradient calculations appear more sensitive to particle number than the microfield calculations. Furthermore, the microcanonical and isokinetic ensembles have a rms difference of 1.0% over the range $\epsilon=0-6$ for $N=686$ with a maximum difference in that range of 2.4%. Thus the results are shown to be relatively insensitive to the choice of ensemble.

IV. RESULTS AND CONCLUSIONS

A comparison between field gradients computed by APEX, NN models, and MD simulations has been carried out for a pure Ar^{+17} plasma at 800 eV at $n_e=10^{24}$ and 10^{25} cm^{-3}. The MD simulation was performed in the microcanonical ensemble with 686 particles. The microcanonical temperature was determined by the relation $k_BT\equiv m\langle v^2\rangle/3$.

Figure 3 shows the results for $n_e=10^{24}$ cm^{-3}. The MD temperature was computed to be 806 eV with a standard deviation (fluctuation) of 11 eV for these results. The error associated with a finite trajectory length in the MD simulation was estimated by fitting a smooth polynomial (fourth or fifth order) through the data and computing the rms fluctuation about the smooth fit. The fluctuations were found to be 0.8% for $\langle\partial_x E_x\rangle_\epsilon$ and 0.3% for $\langle\partial_z E_z\rangle_\epsilon$. The Monte Carlo (MC) calculations of Demura *et al.* [15] for $\langle\partial_z E_z\rangle_\epsilon$, performed in the canonical ensemble, are shown and are in good agreement with our MD results. The interesting region is spectroscopically below $\epsilon=3$ due to the location of the maximum of the microfield probability function (see Fig. 1). In this region, there is good agreement between APEX and the MD simulation with poorer agreement at larger field values. On the other hand, the NN models for $\langle\partial_z E_z\rangle_\epsilon$ are in closer agreement with the MD results for larger field values than for smaller field values, while the NN models for the $\langle\partial_x E_x\rangle_\epsilon$ are in poor agreement with the MD results at all field values studied. In addition screening is relatively unimportant in the NN models for $\langle\partial_x E_x\rangle_\epsilon$ at this temperature and density.

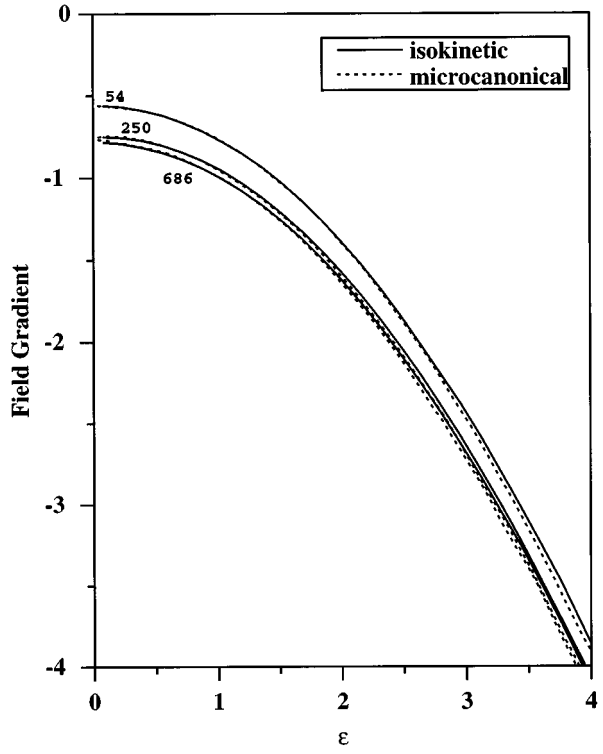

FIG. 2. Field gradients $\langle\partial_z E_z\rangle_\epsilon$ for $N=54$, 250, and 686 particles in the isokinetic and microcanonical ensembles. Sensitivity to the number of particles is much greater for the field gradients than for the microfield distribution. Plasma conditions are the same as in Fig. 1. Field gradients are measured in units of e/r_e^3 and the electric field ϵ is measured in units of e/r_e^2.

Figure 4 shows the results for $n_e=10^{25}$ cm^{-3}. For this case, the MD temperature was computed to be 804 eV with a standard deviation (fluctuation) of 11 eV. The errors associated with a finite trajectory length were found to be 2.3% for $\langle\partial_x E_x\rangle_\epsilon$ and 0.3% for $\langle\partial_z E_z\rangle_\epsilon$. At this higher density, there is good agreement between APEX and the MD simulation below $\epsilon=2$, which is the important region for line shapes due to the peak of the microfield at $\epsilon=1.25$. The NN models again show poor agreement with the MD results at the lower field values. At high field values, we see that for $\langle\partial_z E_z\rangle_\epsilon$ the APEX, MD simulations and screened NN models are converging. For this case also, screening is unimportant in the NN models for $\langle\partial_x E_x\rangle_\epsilon$.

We have compared several theories of the field-constrained-average field gradient. We have demonstrated that the theory of Demura *et al.* is divergent and does not apply to field-constrained quantities in general. A straightforward application of APEX [5] indicates that for small field

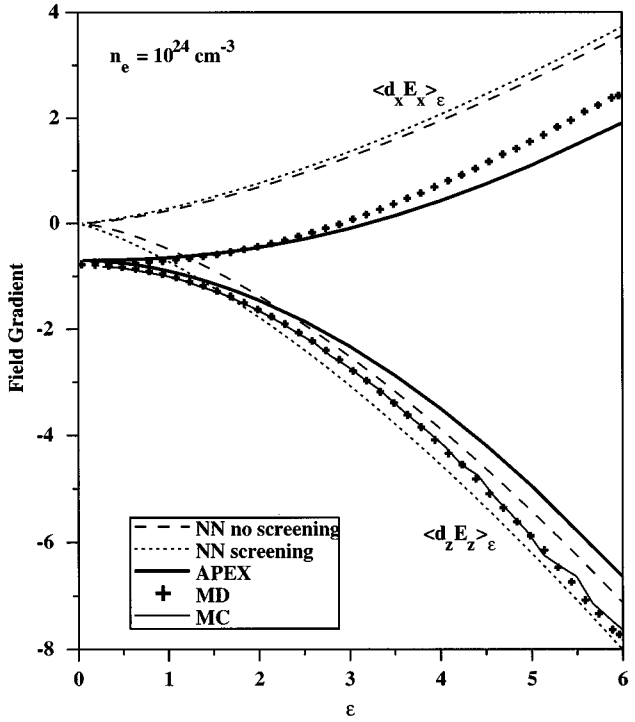

FIG. 3. Field gradients $\langle \partial_x E_x \rangle_\epsilon$ (all plots curving upward) and $\langle \partial_z E_z \rangle_\epsilon$ (all plots curving downward) for $n_e = 10^{24}$ cm^{-3} and $T = 800$ eV. Shown are results obtained from APEX calculation, the nearest-neighbor models, and the MD simulation (done in the microcanonical ensemble). The thin solid line is the MC result of Demura *et al.* Units are the same as in Fig. 2.

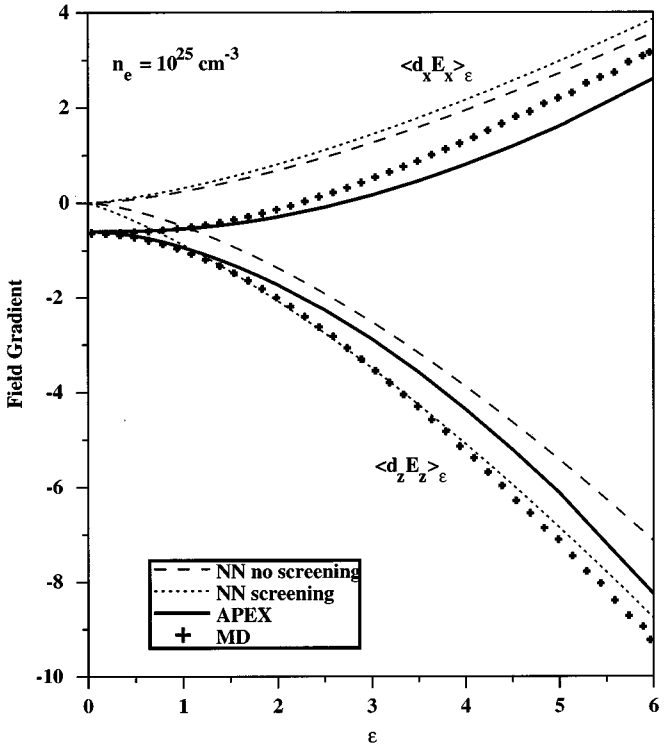

FIG. 4. Same as Fig. 3, but with $n_e = 10^{25}$ cm^{-3}. No MC results were available for this case. Units are the same as in Fig. 2.

values the APEX method accurately gives the part of $g(\mathbf{r}, \boldsymbol{\epsilon})$ sampled in the $\langle \partial_x E_x \rangle_\epsilon$ and $\langle \partial_z E_z \rangle_\epsilon$ averages. At larger field values the agreement between APEX and the MD simulation is not as good and a better theory for $g(\mathbf{r}, \boldsymbol{\epsilon})$ may be needed for applications that require accurate results at these larger field values. The APEX approximation to the field gradients appears, therefore, to be quite satisfactory for spectroscopic applications since the microfield peaks at relatively low field values. A quantitative comparison with experimental line shapes requires a careful consideration of other effects that produce line asymmetries such as the quadratic Stark effect and the presence of satellite lines. In the context of field gradients, we have shown that simple NN models are not accurate at either density for the $\langle \partial_x E_x \rangle_\epsilon$ component and at low field values for both the $\langle \partial_x E_x \rangle_\epsilon$ and $\langle \partial_z E_z \rangle_\epsilon$ components, by comparison with the MD results. The latter result is expected since many-body effects dominate the microfield at low field values and a more sophisticated NN is needed [16]. There does appear to be fairly good agreement between the screened NN model and the MD results, which suggests that the NN limit may be reached at smaller field values for $\langle \partial_z E_z \rangle_\epsilon$ than the $\langle \partial_x E_x \rangle_\epsilon$ component. However, this may simply be fortuitous agreement, and a careful theoretical analysis, which would be beyond the scope of this Brief Report, is needed to ascertain which is the case.

[1] H. R. Griem, Phys. Fluids B **4**, 2346 (1992).
[2] J. W. Dufty, in *Strongly Coupled Plasma Physics*, edited by F. J. Rogers and H. E. DeWitt (Plenum, New York, 1987), p. 493.
[3] J. Halenka, J. Quant. Spectrosc. Radiat. Transfer **39**, 347 (1988).
[4] R. F. Joyce *et al.*, Phys. Rev. A **35**, 2228 (1987). We note that the work of Joyce *et al.* contains a numerical error in the calculation of the constrained average. This error was corrected in Ref. [2].
[5] D. P. Kilcrease *et al.*, Phys. Rev. E **48**, 3901 (1993).
[6] A. V. Demura *et al.*, J. Quant. Spectrosc. Radiat. Transfer **54**, 123 (1995).
[7] J. W. Dufty and L. Zogaib, in *Strongly Coupled Plasma Physics*, edited by S. Ichimaru (North Holland, Amsterdam, 1990).
[8] A. V. Demura, Zh. Éksp. Teor. Fiz. **110**, 114 (1996) [JETP **83**, 60 (1996)].
[9] D. Haynes and C. F. Hooper, Jr. (private communication).
[10] C. A. Iglesias *et al.*, Phys. Rev. A **31**, 1698 (1985).
[11] F. Lado and J. D. Dufty, Phys. Rev. A **36**, 2333 (1987).
[12] J. W. Dufty *et al.*, Phys. Rev. A **31**, 1681 (1985).
[13] J. M. Haile, *Molecular Dynamics Simulation* (Wiley-Interscience, New York, 1992).
[14] M. P. Allen and D. J. Tildesley, *Computer Simulation of Liquids* (Oxford University Press, Oxford, 1994).
[15] D. Gilles kindly provided us with the Monte Carlo results.
[16] C. A. Iglesias *et al.*, Phys. Rev. A **28**, 361 (1983).